



## ShakeOut-D: Ground motion estimates using an ensemble of large earthquakes on the southern San Andreas fault with spontaneous rupture propagation

K. B. Olsen,<sup>1</sup> S. M. Day,<sup>1</sup> L. A. Dalguer,<sup>2</sup> J. Mayhew,<sup>1</sup> Y. Cui,<sup>3</sup> J. Zhu,<sup>3</sup>  
V. M. Cruz-Atienza,<sup>4</sup> D. Roten,<sup>1</sup> P. Maechling,<sup>5</sup> T. H. Jordan,<sup>5</sup> D. Okaya,<sup>5</sup>  
and A. Chourasia<sup>3</sup>

Received 27 November 2008; revised 14 January 2009; accepted 16 January 2009; published 19 February 2009.

[1] We simulate ground motion in southern California from an ensemble of 7 spontaneous rupture models of large ( $M_w$  7.8) northwest-propagating earthquakes on the southern San Andreas fault (ShakeOut-D). Compared to long-period spectral accelerations from the Next Generation Attenuation (NGA) empirical relations, ShakeOut-D predicts similar average rock-site values (i.e., within roughly their epistemic uncertainty), but significantly larger values in Los Angeles and Ventura basins due to wave-guide focusing effects. The ShakeOut-D ground motion predictions differ from those of a kinematically parameterized, geometrically similar, scenario rupture: (1) the kinematic rock-site predictions depart significantly from the common distance-attenuation trend of the NGA and ShakeOut-D results and (2) ShakeOut-D predictions of long-period spectral acceleration within the basins of the greater Los Angeles area are lower by factors of 2–3 than the corresponding kinematic predictions. We attribute these differences to a less coherent wavefield excited by the complex rupture paths of the ShakeOut-D sources. **Citation:** Olsen, K. B., et al. (2009), ShakeOut-D: Ground motion estimates using an ensemble of large earthquakes on the southern San Andreas fault with spontaneous rupture propagation, *Geophys. Res. Lett.*, 36, L04303, doi:10.1029/2008GL036832.

### 1. Introduction

[2] The southern portion of the San Andreas Fault (SAF), between Cajon Creek and Bombay Beach (see Figure 1), has not seen a major event since 1690, and has accumulated a slip deficit of 5–6 meters [Weldon et al., 2004]. The potential for this portion of the fault to rupture in an earthquake with a magnitude as large as  $M_w$  7.8 is a major component of the seismic hazard in southern California and northern Mexico [Field et al., 2008]. Recent simulation efforts (TeraShake-K [Olsen et al., 2006] and TeraShake-D [Olsen et al., 2008]) the suffixes denoting kinematic and

dynamic sources, respectively), modeled 0–0.5 Hz ground motions for an  $M_w$  7.7 earthquake on this fault. The TeraShake-K source, relatively smooth in its slip distribution and rupture characteristics, was derived from inversions of the 2002  $M_w$  7.9 Denali, Alaska, earthquake. The TeraShake-D simulations were carried out with a more complex source derived from spontaneous rupture modeling with small-scale stress-drop heterogeneity. Simulations of northwestward-propagating ruptures, for both TeraShake-K and TeraShake-D sources, predict very intense long-period excitation of sedimentary structures in the Los Angeles region, as a result of a wave-guide effect, i.e., channeling of seismic energy by contiguous basins along the southern edge of the Transverse Ranges. The TeraShake-D models have average values of slip, rupture velocity and slip duration that are nearly the same as the corresponding values for the TeraShake-K sources, and yet the ground motion predictions for the two source types were significantly different. In particular, the TeraShake-D sources decrease the largest peak ground velocities associated with the wave guides and deep basin amplification by factors of 2–3, as compared to those from TeraShake-K. This general reduction in overall ground motion results was mainly attributed to a less coherent wavefield.

[3] The Great Southern California ShakeOut exercise was developed by the USGS [Jones et al., 2008] in order to improve public awareness and readiness for the next great earthquake along the southern SAF. The exercise defined a geologically plausible  $M_w$  7.8 earthquake scenario and a kinematic source description (ShakeOut V1.2 of *Hudnut et al.* [2008] and used for computation of the long-period ground motion component of *Graves et al.* [2008]), here referred to as ShakeOut-K, in which the slip distribution adheres to geologically plausible (“slip predictable”) ranges. To examine whether the findings from the TeraShake study apply to ShakeOut we here present ground motions for spontaneous rupture models conditioned (through the specification of the dynamic stress drop distributions) to have static slip distributions similar to that of the ShakeOut-K source. We then compare the mean and variance of the ground motions for 7 dynamic rupture models (referred to in the following as ShakeOut-D) to those from ShakeOut-K.

### 2. Basin Model, Numerical Methods, and Earthquake Scenarios

[4] The geographical extent of the ShakeOut-D and ShakeOut-K ground motion simulations is shown in Figure 1.

<sup>1</sup>Department of Geological Sciences, San Diego State University, San Diego, California, USA.

<sup>2</sup>Institute of Geophysics, ETH-Zurich, Zurich, Switzerland.

<sup>3</sup>San Diego Supercomputer Center, University of California, San Diego, La Jolla, California, USA.

<sup>4</sup>Instituto de Geofísica, Universidad Nacional Autónoma de México, México, D.F., Mexico.

<sup>5</sup>Department of Earth Sciences, University of Southern California, Los Angeles, California, USA.

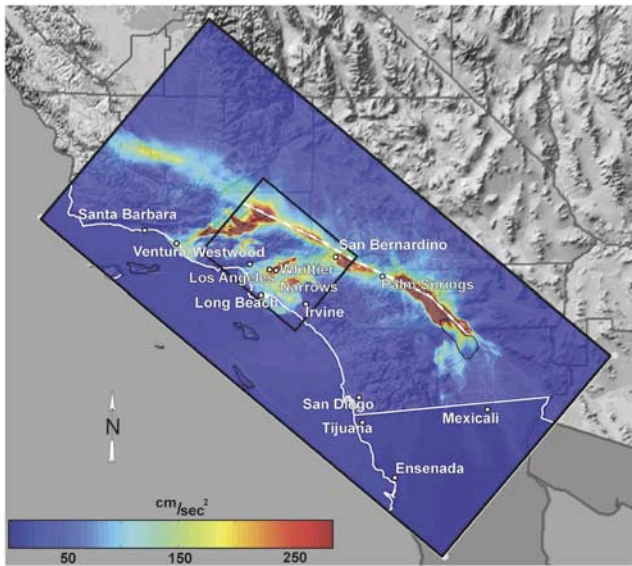


**Figure 1.** Location map for the ShakeOut-D simulations. The large rectangle (121W, 34.5N; 118.9511292W, 36.621696; 116.032285W, 31082920N; 113.943965W, 33.122341N) depicts the simulation area with the mean ShakeOut-D 3s-SAs superimposed. The small rectangle depicts a section used for SA display in Figure 3. The dashed line depicts the part of the SAF that ruptured in the ShakeOut-D simulations.

The 3D crustal structure was obtained using an etree database by mapping the large rectangle in Figure 1 to UTM coordinates for the SCEC Community Velocity Model (CVM) V.4 (<http://epicenter.usc.edu/cmeportal/cmodels.html>) where the lowest S-wave velocity was truncated at 500 m/s.  $Q_s$  was taken as  $50V_s$  ( $V_s$  in km/s), and  $Q_p = 2Q_s$ . Alternative 3D CVMs for southern California should be included in future studies to address the uncertainty in the crustal structure. The dynamic rupture modeling used the staggered-grid split-node (SGSN) scheme [Dalguer and Day, 2007], and the wave propagation was simulated by a 4th-order finite-difference (FD) method [Olsen et al., 2006, 2008], successfully tested against other numerical codes for the ShakeOut-K scenario [see Bielak et al., 2008]. Surface topography was not included in the simulations. Spatial and temporal discretization intervals were 0.2 km and 0.01 s, respectively.

[5] The SAF geometry for the ShakeOut-D simulations was modeled by four vertical, planar segments (Figure 1) where the length and width of the rupture were 300 km and 16 km, respectively. This is an approximation to the more irregular geometry of the fault defined by the SCEC Community Fault Model (CFM) used in the ShakeOut-K simulations. We used the same approximate, two-step procedure as in the TeraShake-D simulations to compute ground motions for ShakeOut-D [see Olsen et al., 2008]. Each spontaneous rupture simulation is done for a simplified, 300 km-long planar (unsegmented) fault geometry imbedded in a 3D velocity model mapped from the SCEC CVM4.0 (Step 1), and the resulting slip-rate functions are applied as kinematic conditions on the 4-segment fault in a second simulation (Step 2). Based on Day et al. [2008], we

estimate that the 0.2 km meshing gives  $\sim 10\%$  accuracy in the Fourier spectrum of ground motion up to  $\sim 0.5$  Hz, and we therefore low-pass filter the slip-rate functions from Step 1 to 0.5 Hz prior to Step 2. We modeled the ShakeOut-K source [Hudnut et al., 2008] for comparison using the irregular fault geometry defined by the SCEC CFM.

### 3. ShakeOut-D Rupture Modeling

[6] Each ShakeOut-D dynamic source was modeled via a slip-matching technique constraining the initial (shear and normal) stress conditions [Dalguer et al., 2008]. This technique allowed us to iteratively perform kinematic and dynamic simulations to find initial distributions that approximately conform to the ShakeOut static slip description of Hudnut et al. [2008]. The ShakeOut-D slip-matching approach also perturbed the initial conditions so as to generate stochastic irregularities compatible with seismological observations [e.g., Mai and Beroza, 2002], similar to the irregularities imposed kinematically in ShakeOut-K. The stochastic irregularities in the rupture models were derived from either Gaussian (correlation lengths of 10 km along strike and 5 km along dip) or Von Karman (correlation lengths of 30 km along strike and 5 km along dip, with Hurst exponents between 0.8 and 1.0) slip models. The distributions of depth-integrated moment density (see Figure 2) all reproduce the ShakeOut scenario relatively well (everywhere within 10% of the ShakeOut uncertainty range specified by Hudnut et al. [2008]; by comparison, ShakeOut-K has fluctuations up to  $\sim 30\%$  outside that range). As Figure 2 illustrates, 4 of the 7 dynamic rupture models vary greatly in their fault-plane spatial-temporal distributions of final slip and rupture time, even though averages are nearly identical. The remaining 3 ShakeOut-D sources are variants of the rupture model ‘g3d7’, with initial stress conditions that yielded similar slip (but somewhat different slip-rate distributions).

### 4. ShakeOut-D Wave Propagation

[7] The dynamic sources were used (in step 2) to simulate wave propagation within the 600 km by 300 km area shown in Figure 1 to a depth of 80 km. The mean of the spectral accelerations at a period of 3 s (3s-SAs) with 5% damping from ShakeOut-D is shown in Figure 1 for the entire model area and in Figure 3 for the greater Los Angeles area. In addition, Figure 3 shows the (upper) standard deviation  $\sigma$  of the ShakeOut-D 3s-SA values, as well the 3s-SA values for our ShakeOut-K simulation. The mean ShakeOut-D and ShakeOut-K 3s-SA patterns contain the same overall features as for the TeraShake1–2 results reported by Olsen et al. [2006, 2008], such as rupture directivity, a localized amplification area near Whittier Narrows (WN), and another just south of WN (south of the Puente Hills), due to waveguides focusing seismic energy. As for TeraShake the (northern) wave guide through WN generates the strongest amplification of the two wave guides. Furthermore, strong amplification is generated along the southern part of the rupture segment, and in the San Bernardino basin (see Figure 1). However, additional areas of elevated ground motions are generated toward the north for ShakeOut-D (and for ShakeOut-K) due to a (33%) longer fault rupture as

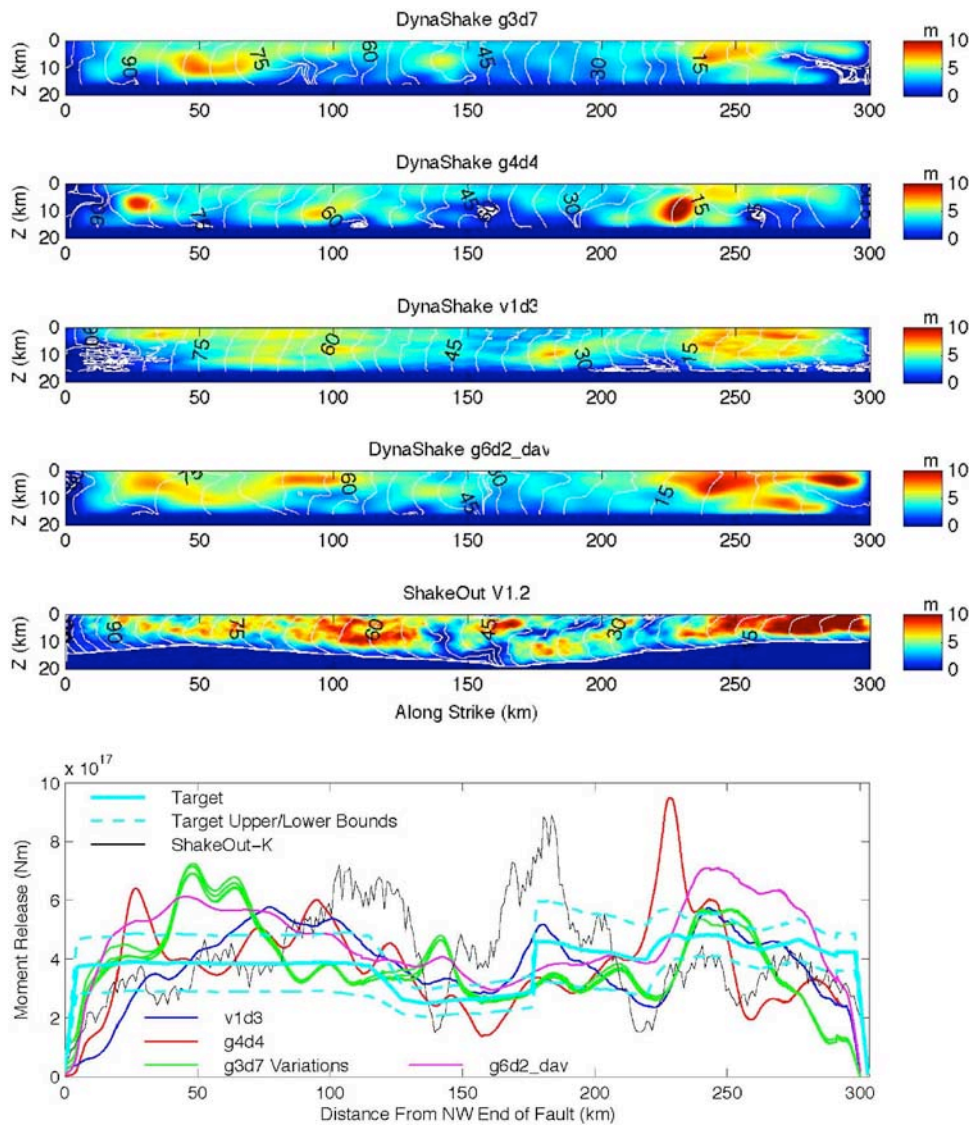


**Figure 2.** (top) Slip distributions for 4 of the 7 ShakeOut-D sources and ShakeOut-K. The white contours and contour labels depict the rupture times. (bottom) Distributions of depth-integrated moment density along the fault.

compared to TeraShake. In particular, additional waveguide-like channeling occurs near the northern end of the ShakeOut rupture, extending west into the Ventura basin, with strong localized amplification. Not surprisingly, the largest standard deviations ( $\sigma$ s) associated with the ensemble mean 3s-SA values in the greater Los Angeles area are found along the wave guides (the excitation of which is sensitive to rupture directivity) and within some of the other basin areas (see Figure 3).

[8] Another result consistent with those from TeraShake is the general reduction in ground motion extremes of the ShakeOut-D simulations away from the fault, as compared to those from ShakeOut-K. For example, the ShakeOut-D has mean 3s-SA values that are smaller than those from ShakeOut-K by up to a factor of 3 in the basin and wave guide amplification areas of greater Los Angeles (see Figure 3). Figure 4a compares the ensemble mean 3s-SA values for ShakeOut-D to ShakeOut-K at 12 selected sites. The waveguide maximum (WN) and deep basin (Down) sites for ShakeOut-D are reduced by factors of 2.2 and 2.1, respec-

tively, as compared to ShakeOut-K. At locations with concentrations of high-rise buildings, such as downtown Los Angeles (LADT), Century City, downtown Burbank (dt Burbank), and Wilshire and Western (W&W), typically on shallower sediments and away from the principal zones influenced by the convergent guided waves, the mean ShakeOut-D 3s-SAs are also smaller than those from ShakeOut-K, by up to a factor of 3.2. The 3s-SA for ShakeOut-K at the northern wave guide (Pard) is 25% larger than the mean ShakeOut-D.

[9] Figure 4b compares 3s-SA values for the mean of the ShakeOut-D ensemble with those of our ShakeOut-K simulation, at all rock sites within 200 km of the fault rupture. The rock sites were defined by a surface  $V_s > 1000$  m/s for ShakeOut-D (the SCEC CVM does not include a weathered layer for rock sites, which would reduce these surficial  $V_s$  values by a factor of 2 to 3 without significantly affecting 3s-SAs, as argued by, e.g., Day *et al.* [2008]). The rock-site distance dependences of ShakeOut-K and ShakeOut-D are very different. While the medians agree well for distances



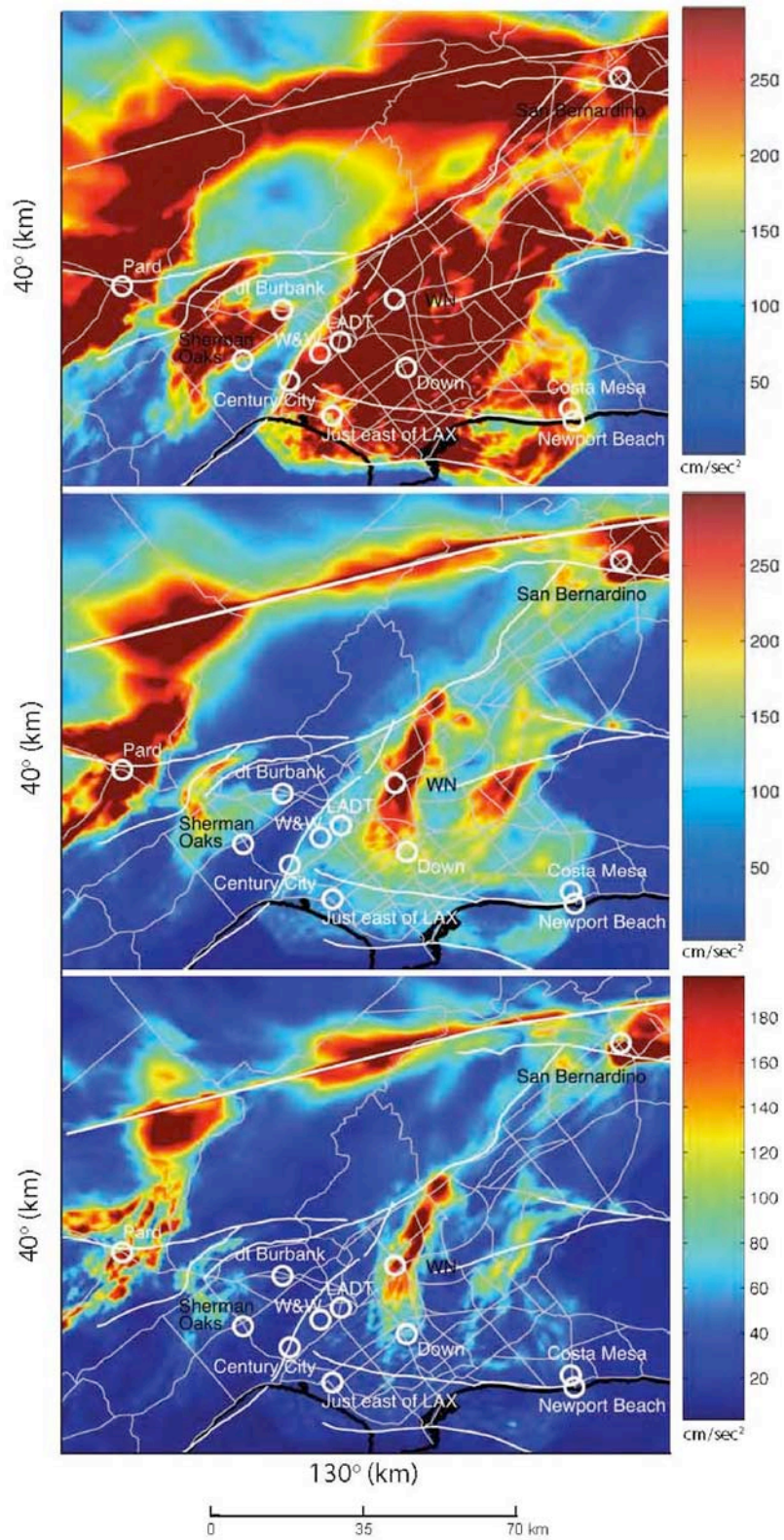


**Figure 3.** The 3s-SA for (top) ShakeOut-K and (middle) mean of ShakeOut-D within the area depicted by the small rectangle in Figure 1. (bottom) The  $\sigma$  for ShakeOut-D.

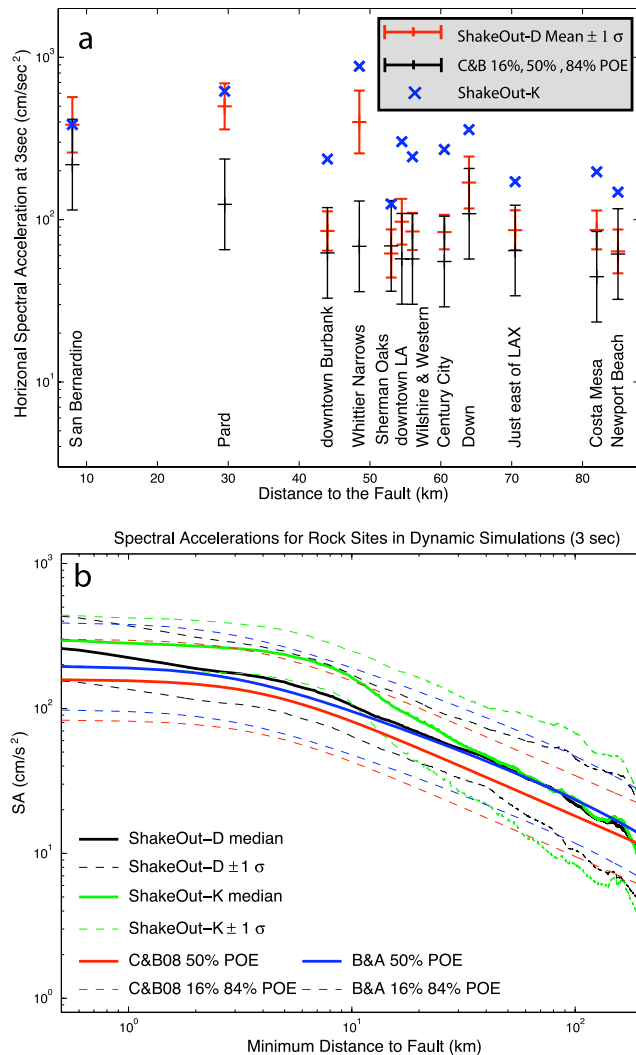


**Figure 4.** Comparison between 3s-SA at rock sites (a) for 12 selected sites and (b) for the mean of ShakeOut-D, for ShakeOut-K, and for CB08 and BA08.

less than about 1 km and larger than about 30 km from the fault, the ShakeOut-K medians are up to 60% larger than those from ShakeOut-D between 1 km and 30 km from the fault. The larger values for ShakeOut-K in this range must reflect characteristics of the ShakeOut-K source model that differ systematically from the ShakeOut-D ensemble. A possible source of this difference would be the presence of strong rupture-induced directivity in ShakeOut-K. Strong directivity in ShakeOut-K would concentrate intense motions relatively near the fault, but might have diminishing effect at the very closest distances, because the ShakeOut-K source model has reduced rupture velocities along the top few kilometers of the fault. At greater depths, ShakeOut-K has rupture velocities that are often near or above the Rayleigh velocity (see Figure 2). In contrast, rupture-front coherence, and therefore directivity effects, are likely to be substantially reduced by the complex dynamic ruptures that emerge in the ShakeOut-D simulations, compared with the ShakeOut-K source. Moreover, the ShakeOut-D sources satisfy local energy conservation, which puts constraints

on possible rupture velocities (e.g., velocities between the Rayleigh and S velocities are precluded in the limit of small cohesive zone [Freund, 1989]) whereas ShakeOut-K, being kinematically prescribed, need not obey those energy constraints.

## 5. Comparison With Empirical Relations

[10] In this section we compare ShakeOut-D 3s-SAs with those from attenuation relationships (ARs) proposed by Campbell and Bozorgnia [2008] (hereinafter referred to as CB08) and by Boore and Atkinson [2008] (hereinafter referred to as BA08). Note that CB08 includes a depth-dependent basin amplification correction term while BA08 does not. Figure 4a includes 3s-SA values from the CB08 attenuation relation at the 12 selected sites discussed in the previous section (see Figure 3 for location). The mean 3s-SA for ShakeOut-D is between two and three  $\sigma$ s above the CB08 median (i.e. between the 0.1–0.2% and 2% probability of exceedance, POE) at WN near the junction between Los Angeles and San Gabriel basins and at the deep basin site Downey. The 3s-SA for the mean ShakeOut-D at the northern wave guide (Pard) is at about the median plus  $2\sigma$  for CB08. At the 9 locations of high-rise buildings, all ShakeOut-D 3s-SA values are within  $1\sigma$  of the empirical median levels, versus 2 to  $3\sigma$  above the empirical median for ShakeOut-K (all relative to CB08).

[11] Figure 4b, in addition to showing the 3s-SA rock-site medians from ShakeOut-D and ShakeOut-K, also shows the corresponding rock-site values for CB08 and BA08 (computed using an average depth of 400 m to the  $V_s = 2500$  m/s isosurface for CB08, and with the simplification that  $V_{s30} = 760$  m/s). The 3s-SA values predicted from BA08 are 17–31% larger than those from CB08 and are very close to the values from the ShakeOut-D simulations (within  $\sim 10\%$  for all distances from 2–100 km, and within  $\sim 30\%$  at distances  $\sim 1$  km and less).

[12] Since all ShakeOut-D simulations have slip distributions matched (at long wavelength) to the ShakeOut scenario, the ensemble does not capture the source variability we would expect for M7.8 events in general. Therefore, the ShakeOut-D  $\sigma$ s in Figure 4b represent principally intra-event variability of SA, and they should be compared with the intra-event component of  $\sigma$  for the ARs (which are smaller than the total AR  $\sigma$ s derived by combining intra-event and inter-event components). For  $\ln(3s-SA)$ , the ShakeOut-D  $\sigma$ s are very close to  $\sim 0.5$  at all distances up to 50 km. This value compares favorably with intra-event  $\sigma$ s of  $\sim 0.56$  for both BA08 and CB08. The  $\sigma$ s for ShakeOut-D increase significantly for distances beyond 50 km, reaching  $\sim 0.7$  at 100 km. The ShakeOut-K  $\sigma$  is small,  $\sim 0.39$ , for distances less than 10 km, but increases rapidly thereafter, and is significantly larger than that of ShakeOut-D (and the empirical ARs) for all distances greater than  $\sim 15$  km.

## 6. Discussion and Conclusions

[13] A possible explanation for the reduction of ground motion extremes in the Los Angeles area for the ShakeOut-D sources, relative to ShakeOut-K (Figure 4), is less coherent rupture of the ShakeOut-D sources. The differences in wavefield coherency may be caused by strong local fluctu-

ations (abruptness of changes in direction and speed in the rupture propagation) in the spontaneous-rupture sources but lacking in the kinematic sources, as proposed by Olsen *et al.* [2008]. Graves *et al.* [2008] demonstrate that predicted ground motions in Los Angeles are significantly reduced if one introduces relatively moderate reductions in the average rupture speed of the ShakeOut-K scenario. It is possible that this sensitivity reflects, in part, the presence in ShakeOut-K of segments rupturing at velocities between the local Rayleigh and S-wave velocities, i.e., the range that is energetically precluded. Dynamically simulated sources will naturally avoid the energetically-precluded regime.

[14] The ShakeOut-K/ShakeOut-D comparison shows that both kinematic and dynamic simulations can capture geology-specific path effects that may have large impact on seismic hazard at some sites (as with the sedimentary channeling effect discussed here). Simulation ensembles thus have the potential to greatly improve Probabilistic Seismic Hazard Analysis. However, the strong rupture-velocity sensitivity noted by Graves *et al.* [2008] raises the concern that kinematic parameterization of the source (in which rupture velocity is specified without direct constraints from rupture dynamics) may lead to large variances in ensemble estimates. In contrast, the relative stability of the ShakeOut-D predictions (at a given site) suggests that simulation ensemble variances may be substantially reduced through use of sources based on spontaneous rupture simulations, which should be tested in future work by adding more scenarios. Alternatively, kinematic source parameterizations should be improved to better incorporate constraints from those simulations.

[15] **Acknowledgments.** This work is funded through NSF grants including (1) Petascale Cyberfacility for Physics-based Seismic Hazard Analysis Research Project (PetaSHA) (EAR-0623704) and (2) Enabling Earthquake System Science through Petascale Calculations (PetaShake) (OCI-749313). This is SCEC publication 1255.

## References

- Bielak, J., et al. (2008), ShakeOut simulations: Verification and comparisons, paper presented at SCEC Annual Meeting, South. Calif. Earthquake Cent., Palm Springs.
- Boore, D. M., and G. M. Atkinson (2008), Ground-motion prediction equations for the average horizontal component of PGA, PGV, and 5%-damped PSA at spectral periods between 0.01 s and 10.0 s, *Earthquake Spectra*, 24, 99–138.
- Campbell, K. W., and Y. Bozorgnia (2008), NGA ground motion model for the geometric mean horizontal component of PGA, PGV, PGD and 5% damped linear elastic response spectra for periods ranging from 0.01 to 10 s, *Earthquake Spectra*, 24, 139–171.
- Dalguer, L. A., and S. M. Day (2007), Staggered-grid split-node method for spontaneous rupture simulation, *J. Geophys. Res.*, 112, B02302, doi:10.1029/2006JB004467.
- Dalguer, L. A., S. M. Day, K. Olsen, and V. M. Cruz-Atienza (2008), Rupture models and ground motion for ShakeOut and other southern San Andreas fault scenarios, paper presented at 14th World Conference on Earthquake Engineering, Int. Assoc. for Earthquake Eng., Beijing.
- Day, S. M., R. W. Graves, J. Bielak, D. Dreger, S. Larsen, K. B. Olsen, A. Pitarka, and L. Ramirez-Guzman (2008), Model for basin effects on long-period response in southern California, *Earthquake Spectra*, 24, 257–277.
- Field, E. H., et al. (2008), The uniform California earthquake rupture forecast, version 2 (UCERF 2), *U.S. Geol. Surv. Open File Rep.*, 2007–1437.
- Freund, L. B. (1989), *Dynamic Fracture Mechanics*, Cambridge Univ. Press, New York.
- Graves, R. W., B. Aagaard, K. Hudnut, L. Star, J. Stewart, and T. H. Jordan (2008), Broadband simulations for *M<sub>w</sub>* 7.8 southern San Andreas earthquakes: Ground motion sensitivity to rupture speed, *Geophys. Res. Lett.*, 35, L22302, doi:10.1029/2008GL035750.
- Hudnut, K. W., B. Aagaard, R. Graves, L. Jones, T. Jordan, L. Star, and J. Stewart (2008), ShakeOut earthquake source description, surface faulting and ground motions, *U.S. Geol. Surv. Open File Rep.*, 2008-1150. (Available at <http://pubs.usgs.gov/of/2008/1150/>)
- Jones, L., et al. (2008), The ShakeOut scenario, *U.S. Geol. Surv. Open File Rep.*, 2008–1150.
- Mai, P. M., and G. C. Beroza (2002), A spatial random field model to characterize complexity in earthquake slip, *J. Geophys. Res.*, 107(B11), 2308, doi:10.1029/2001JB000588.
- Olsen, K. B., S. M. Day, J. B. Minster, Y. Cui, A. Chourasia, M. Faerman, R. Moore, P. Maechling, and T. H. Jordan (2006), Strong shaking in Los Angeles expected from southern San Andreas earthquake, *Geophys. Res. Lett.*, 33, L07305, doi:10.1029/2005GL025472.
- Olsen, K. B., S. M. Day, J. B. Minster, Y. Cui, A. Chourasia, D. Okaya, P. Maechling, and T. H. Jordan (2008), TeraShake2: Simulation of *M<sub>w</sub>* 7.7 earthquakes on the southern San Andreas fault with spontaneous rupture description, *Bull. Seismol. Soc. Am.*, 98, 1162–1185, doi:10.1785/0120070148.
- Weldon, R., K. Scharer, T. Fumal, and G. Biasi (2004), Wrightwood and the earthquake cycle: What a long recurrence record tells us about how faults work, *Geol. Seismol. Am. Today*, 14, 4–10.
- A. Chourasia, Y. Cui, and J. Zhu, San Diego Supercomputer Center, University of California, San Diego, 9500 Gilman Drive, La Jolla, CA 92023, USA.
- V. M. Cruz-Atienza, Instituto de Geofísica, Universidad Nacional Autónoma de México, C. P. 04150, México, D.F., Mexico.
- L. A. Dalguer, Institute of Geophysics, ETH-Zurich, CH-8093 Zurich, Switzerland.
- S. M. Day, J. Mayhew, K. B. Olsen, and D. Roten, Department of Geological Sciences, San Diego State University, San Diego, CA 92182, USA. (kbolsen@sciences.sdsu.edu)
- T. H. Jordan, P. Maechling, and D. Okaya, Department of Earth Sciences, University of Southern California, Los Angeles, CA 90089-0740, USA.